ISBN: 978-3-95450-214-1 ISSN: 2673-5490 doi:10.18429/JACoW-IPAC2021-TUPAB249

DIFFRACTION AT THE OPEN-ENDED DIELECTRIC-LOADED CIRCULAR WAVEGUIDE*

S. N. Galyamin†, A. V. Tyukhtin, St. Petersburg State University, St. Petersburg, Russia
V. V. Vorobev, Technical University of Munchen, Munchen, Germany

Abstract

First, radiation at the open end of a dielectric-loaded circular waveguide is investigated. Rigorous solution obtained via the modified tayloring technique is presented, both far-field and near-field distribution is illustrated. Second, dielectric-lined case and the case of shallow corrugation of the inner waveguide wall are solved using the same approach. Applications of the discussed structures lie in the area of THz-driven bunch manipulation, wakefield acceleration and beam-driven THz sources.

INTRODUCTION

In recent years, much attention has been paid to the open-ended waveguide structures with different dielectric fillings (or corrugation which is in certain sence equivalent to certain filling [1]) due to a number of promising applications such as dielectric wakefield acceleration [2], THz-driven bunch compression, streaking [3, 4] and beam-driven narrow-band THz sources [5–7].

Almost all the mentioned cases involve interaction of both THz waves and charged particle bunches with an open end of certain waveguide structure loaded with dielectric, most frequently a circular capillary. For further development of the discussed prospective topics a coresponding rigorous approach is necessary, such an approach has been presented recently [8]. Here we briefly explain the main steps of this method and show several representative examples for dielectric-loaded, dielecric-lined and shallow-corrugated open-ended wave guides driven by an incident waveguide mode.

OPEN-ENDED WAVEGUIDE WITH UNIFORM DIELECTRIC FILLING

We consider a semi-infinite cylindrical waveguide with radius a filled with a dielectric ($\varepsilon > 1$) (Fig. 1) and suppose that single TM_{0l} waveguide mode incidents the orthogonal open end (we are working in the frequency domain):

$$H^{(i)}_{\omega\varphi} = M^{(i)} J_1(\rho j_{0l}/a) e^{i k_{zl} z}, \tag{1}$$

where $M^{(i)}$ is an arbitrary amplitude constant for the incident mode, J_ν is a Bessel function of ν-th order, $J_0(j_{0l}) = 0$, $k_{zl} = \sqrt{k_0^2\varepsilon - j_{0l}^2 a^{-2}}$, $\operatorname{Im} k_{zl} > 0$, $k_0 = \omega/c + i\delta$ ($\delta \to 0$, which is equivalent to infinitely small dissipation an all areas), c is the light speed in vacuum. It should be noted that wavegude walls are supposed to have an ideal electric conductivity, therefore $E_{\omega z} = 0$ for $\rho = a$, $z < 0$.

* Work supported by Russian Science Foundation, Grant No. 18-72-10137
† s.galyamin@spbu.ru

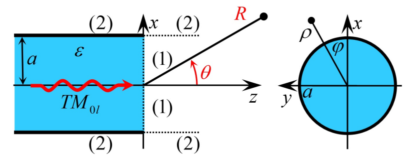

Figure 1: Geometry of the problem and main notations.

The reflected field in the area $z < 0$, $\rho < a$ is decomposed into a series of waveguide modes propagating in opposite direction:

$$H^{(r)}_{\omega\varphi} = \sum\nolimits_{m=1}^{\infty} M_m J_1(\rho j_{0m}/a) e^{-i k_{zm} z}, \tag{2}$$

where $\{M_m\}$ are unknown "reflection coefficients" that should be determined. The vacuum area is divided into two subareas "1" and "2" (see Fig. 1), where we introduce functions $\Phi_\pm(\rho, \alpha)$ (hereafter subscripts $\pm$ mean that function is holomorphic and free of poles and zeros in areas $\operatorname{Im}\alpha > -\delta$ and $\operatorname{Im}\alpha < \delta$, correspondingly), for example:

$$\Phi^{(1,2)}_{+}(\rho, \alpha) = (2\pi)^{-1} \int_0^\infty dz \frac{k_0}{i} E^{(1,2)}_{\omega z}(\rho, z) e^{i\alpha z}, \tag{3}$$

which are the transforms of $E^{(1,2)}_{\omega z}$.

We utilize field matching for $z = 0$, $0 < \rho < a$ and for $\rho = a$, $z > 0$ and arrive at the Wiener-Hopf-Fock equation, formal solution of which (it still contains unknown coefficients M_m) is the following:

$$\begin{aligned} \Phi^{(2)}_{+}(a, \alpha) = &-\frac{\kappa_+(\alpha) G_+(\alpha)}{4\pi} \\ &\times \left[M^{(i)} \eta_{l+}(\alpha) J_1(j_{0l}) - \sum_{m=1}^{\infty} M_m \zeta_{m+}(\alpha) J_1(j_{0m}) \right], \end{aligned} \tag{4}$$

where $\kappa(\alpha) = \sqrt{k_0^2 - \alpha^2}$, $\kappa_+ = \sqrt{k_0 + \alpha}$,

$$\begin{gathered} G(\alpha) = \pi a \kappa J_0(a\kappa) H^{(1)}_0(a\kappa) = G_+(\alpha) G_-(\alpha), \\ \eta_{l+}(\alpha) = \kappa_+(\alpha_l) G_+(\alpha_l) \frac{\frac{k_{zl}}{\varepsilon} + \alpha_l}{2\alpha_l(\alpha_l + \alpha)}, \\ \zeta_{m+}(\alpha) = \kappa_+(\alpha_m) G_+(\alpha_m) \frac{\frac{k_{zm}}{\varepsilon} - \alpha_m}{2\alpha_m(\alpha_m + \alpha)}, \end{gathered} \tag{5}$$

$\alpha_m = \sqrt{k_0^2 - j_{0m}^2 a^{-2}}$, $\operatorname{Im}\alpha_m > 0$ are longitudinal wavenumbers of vacuum waveguide.

To resolve this, one should implement the so-called "regularity condition" which is, in general, the consequence of the fact that physical fields should vanish at the infinity:

$$\begin{aligned} \Phi^{(2)}_{+}(a, \alpha_p) = &\frac{ia}{4\pi} J_1(j_{0p}) \\ &\times \left[\delta_{lp} M^{(i)} \left(\frac{k_{zp}}{\varepsilon} - \alpha_p \right) - M_p \left(\frac{k_{zp}}{\varepsilon} + \alpha_p \right) \right], \end{aligned} \tag{6}$$

Content from this work may be used under the terms of the CC BY 3.0 licence (© 2021). Any distribution of this work must maintain attribution to the author(s), title of the work, publisher, and DOI

ISBN: 978-3-95450-214-1 ISSN: 2673-5490 doi:10.18429/JACoW-IPAC2021-TUPAB249
Content from this work may be used under the terms of the CC BY 3.0 licence (© 2021). Any distribution of this work must maintain attribution to the author(s), title of the work, publisher, and DOI

where $p = 1, 2, \dots$ and δ_{lp} is the Kronecker symbol. Substiting Eq. (4) into Eq. (6) we obtain the following infinite linear system for M_m:

$$\sum_{m=1}^{\infty} W_{pm} M_m = w_p, \quad p = 1, 2, \dots, \tag{7}$$

where

$$W_{pm} = J_1(j_{0m}) \left[\zeta_{m+}(\alpha_p) + \delta_{mp} ia \frac{\frac{k_{zm}}{\varepsilon} + \alpha_m}{\kappa_+(\alpha_m) G_+(\alpha_m)} \right],$$
$$w_p = M^{(i)} J_1(j_{0l}) \left[\eta_{l+}(\alpha_p) + \delta_{lp} ia \frac{\frac{k_{zl}}{\varepsilon} - \alpha_l}{\kappa_+(\alpha_l) G_+(\alpha_l)} \right]. \tag{8}$$

Equation (7) can be solved numerically with arbitrary accuracy using the reducing technique.

For calculations, the mode frequency was chosen to be equal to the frequency of CR mode f_l^{CR} with number l produced by a moving charge having its Lorentz factor $\gamma = 7$:

$$\omega_l^{\mathrm{CR}} = 2\pi f_l^{\mathrm{CR}} = c\beta j_{0l} / \left(a\sqrt{\varepsilon\beta^2 - 1} \right), \tag{9}$$

where $\beta = \sqrt{1 - \gamma^{-2}}$. With this choice, an incident mode (1) corresponds to the l-th mode of a charged particle bunch wakefield if $M^{(i)}$ is chosen appropriately [8]. Figure 2 shows S-parameters calculated via presented rigorous analytical approach and obtained from COMSOL simulations. As one can see, the agreement between results is excellent. Typically, the reflected mode with the number of incident mode dominates ("close to single mode" regime). Figure 3 shows far-field patterns for $l = 5$, 10, 20. One can see that the angle of maximum radiation depends on mode number (this result lies beyond ray-optics consideration) allowing realization of a multi-frequency THz source using single waveguide structure driven by a short bunch.

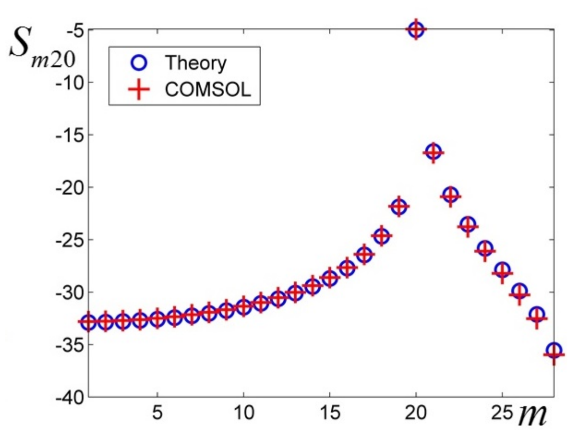

Figure 2: S-parameters (in dB) obtained via the presented analytical approach and via COMSOL simulations: S_{ml} corresponds to frequency f_l^{CR} (9) and incident mode with number l, $f_{20}^{\mathrm{CR}} = 1.247$ THz, $a = 0.24$ cm, $\varepsilon = 2$.

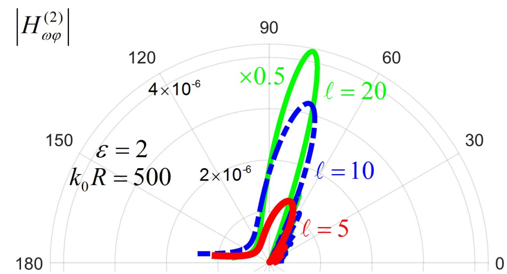

Figure 3: Far-field distribution for the absolute value of $H^{(2)}_{\omega\varphi}$, $R = 500/k_0$, other parameters are the same as in Fig. 2, a number near curves means the number of the exciting CR mode, $M^{(i)}$ is chosen so that a power of each mode equals 1.

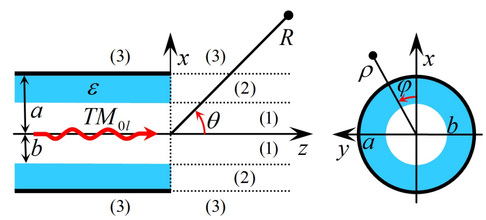

Figure 4: Geometry of a dielectric-lined case.

OPEN-ENDED DIELECTRIC-LINED WAVEGUIDE

Similar approach can be utilized for more complicated case (Fig. 4). Analytical details for this problem can be found in [9]. Numerical results for S-parameters are shown in the left plot of Fig. 5. Compared to the case of uniform filling (Fig. 2), mode structure is more complicated. However, for large enough l the reflected mode with the number of incident mode dominates, therefore the overall diffraction process is similar to a "single-mode" regime (for $l = 5$ or lower other modes can be significant). Concerning the far-field (two right plots in Fig. 5) the following can be noted: for low-order modes (5 and lower), the radiation pattern loses its "single-lobe" form due to the fact that differend modes contribute comparable to the total radiation. For modes with numbers 10 and higher the process is generally the same but the result is different: maxima of numerous narrow lobes lie near the axis of the structure and merge into a single (but wider) lobe.

OPEN-ENDED SHALLOW-CORRUGATED WAVEGUIDE

Finally, a solution is obtained for the problem of diffraction of a waveguide mode at the open end of a circular waveguide with a shallow corrugated rectangular profile on the inner surface, analytical details can be found in [10]. Among the differences from the problem with uniform dielectric filling, the following can be noted: when excited by the Cherenkov mode (this is always the first mode), a multimode regime is typical, which leads to a "multilobe" radiation pattern, see Fig. 6.

ISBN: 978-3-95450-214-1 ISSN: 2673-5490 doi:10.18429/JACoW-IPAC2021-TUPAB249

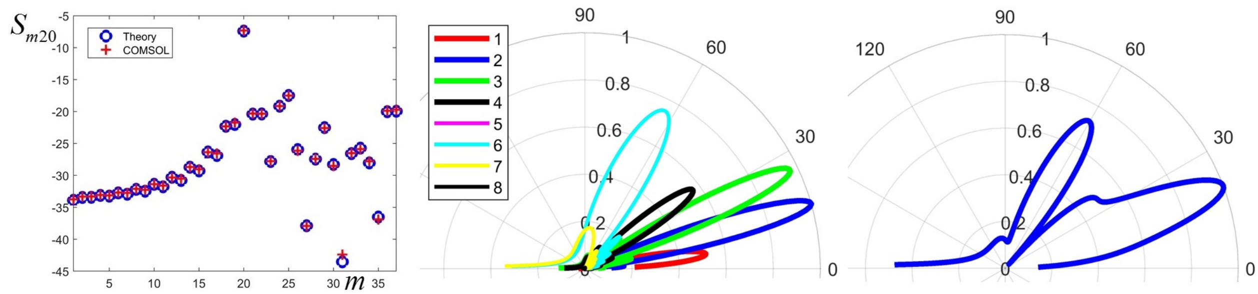

Figure 5: Left plot: S-parameters for $l = 20$ ($f_{20}^{\mathrm{CR}} = 1.81$ THz). Two right plots: far-field (for the absolute value of $H_{\omega\varphi}^{(2)}$), $R = 500/k_0$, $l = 5, f_5^{\mathrm{CR}} = 397$ GHz. Other parameters: $a = 0.24$ cm, $b = a/3$, $\varepsilon = 2$.

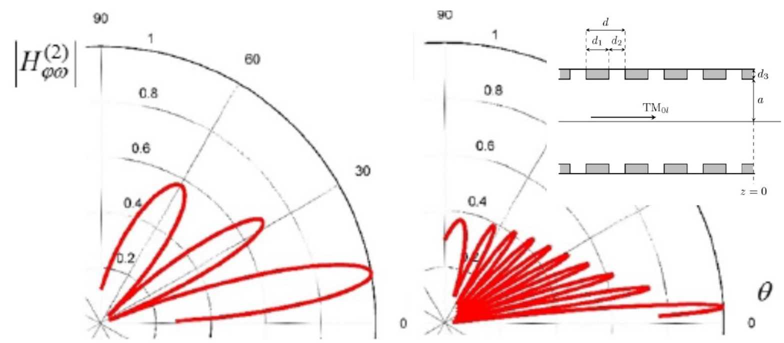

Figure 6: Far-field distribution for the absolute value of $H_{\omega\varphi}^{(2)}$, $R = 1000/k_0$, $a = 0.24$cm, $l = 1$, other parameters: $f = 200$ GHz, $d_1 = 0.005$cm, $d_2 = d_3 = 0.01$cm, $\beta = k_0/k_{z1} = 0.9996$, 3 propagating modes (left), $f = 615$ GHz, $d_1 = d_2 = d_3 = 0.005$cm, $\beta = k_0/k_{z1} = 0.9982$, 10 propagating modes (right).

REFERENCES

[1] G. Stupakov and K. L. F. Bane, "Surface impedance formalism for a metallic beam pipe with small corrugations", *Phys. Rev. ST Accel. Beams*, vol. 15, p. 124401, 2012. doi:10.1103/PhysRevSTAB.15.124401

[2] B. D. O'Shea *et al.*, "Observation of acceleration and deceleration in gigaelectron-volt-per-metre gradient dielectric wakefield accelerators", *Nature Comm.*,vol. 7, p. 12763, 2016. doi:10.1038/ncomms12763

[3] L. Zhao *et al.*, "Femtosecond Relativistic Electron Beam with Reduced Timing Jitter from THz Driven Beam Compression", *Phys. Rev. Lett.*, vol. 124, p. 054802, 2020. doi:10.1103/PhysRevLett.124.054802

[4] E. C. Snively *et al.*, "Femtosecond Compression Dynamics and Timing Jitter Suppression in a THz-driven Electron Bunch Compressor", *Phys. Rev. Lett.*, vol. 124, p. 054801, 2020. doi:10.1103/PhysRevLett.124.054801

[5] D. Wang *et al.*, "Non-perturbing THz generation at the Tsinghua University Accelerator Laboratory 31 MeV electron beamline", *Rev. Sci. Instrum.*, vol. 89, p. 093301, 2018. doi:10.1063/1.5042006

[6] S. N. Galyamin *et al.*, "Terahertz radiation from an ultra-relativistic charge exiting the open end of a waveguide with a dielectric layer", *Optics Express*, vol. 22, p. 8902, 2014. doi:10.1364/OE.22.008902

[7] S. Jiang *et al.*, "Intrinsically reducing divergence angle of Cherenkov radiation from dielectric capillary", *Optics Letters*, vol. 45, p. 5416, 2020. doi:10.1364/OL.401947

[8] S. N. Galyamin *et al.*, "Diffraction at the Open-Ended Dielectric-Loaded Circular Waveguide: Rigorous Approach", *IEEE Trans. Microwave Theory Techn.*, vol. 69, p. 2429, 2021. doi:10.1109/TMTT.2021.3064343

[9] S. N. Galyamin and V. V. Vorobev, "Diffraction at the Open End of Dielectric-Lined Circular Waveguide", 2021. arxiv:2104.12375

[10] S. N. Galyamin and A. A. Grigoreva, "Diffraction of Cherenkov Radiation at the Open End of a Shallow Corrugated Waveguide", 2020. arxiv:2005.05020

© Content from this work may be used under the terms of the CC BY 3.0 licence (© 2021). Any distribution of this work must maintain attribution to the author(s), title of the work, publisher, and DOI